Novel Orange-Yellow-Green Color-tunable Bi^{3+}-doped $Ba_3Y_{4-w}Lu_wO_9$ ($0 \leq w \leq 4$) Luminescence Materials: Site Migration and Photoluminescence Control

Gongcheng Xing,[a] Zhiyu Gao,[a] Mengxuan Tao,[a] Yi Wei,[a] Yixin Liu,[a] Peipei Dang,[b] and Guogang, Li*[a] and Jun Lin*[b]

[a] *Engineering Research Center of Nano-Geomaterials of Ministry of Education, Faculty of Materials Science and Chemistry, China University of Geosciences, 388 Lumo Road, Wuhan 430074, P. R. China. E-mail: ggli@cug.edu.cn*

[b] *State Key Laboratory of Rare Earth Resource Utilization, Changchun Institute of Applied Chemistry, Chinese Academy of Sciences, Changchun 130022, P. R. China.*

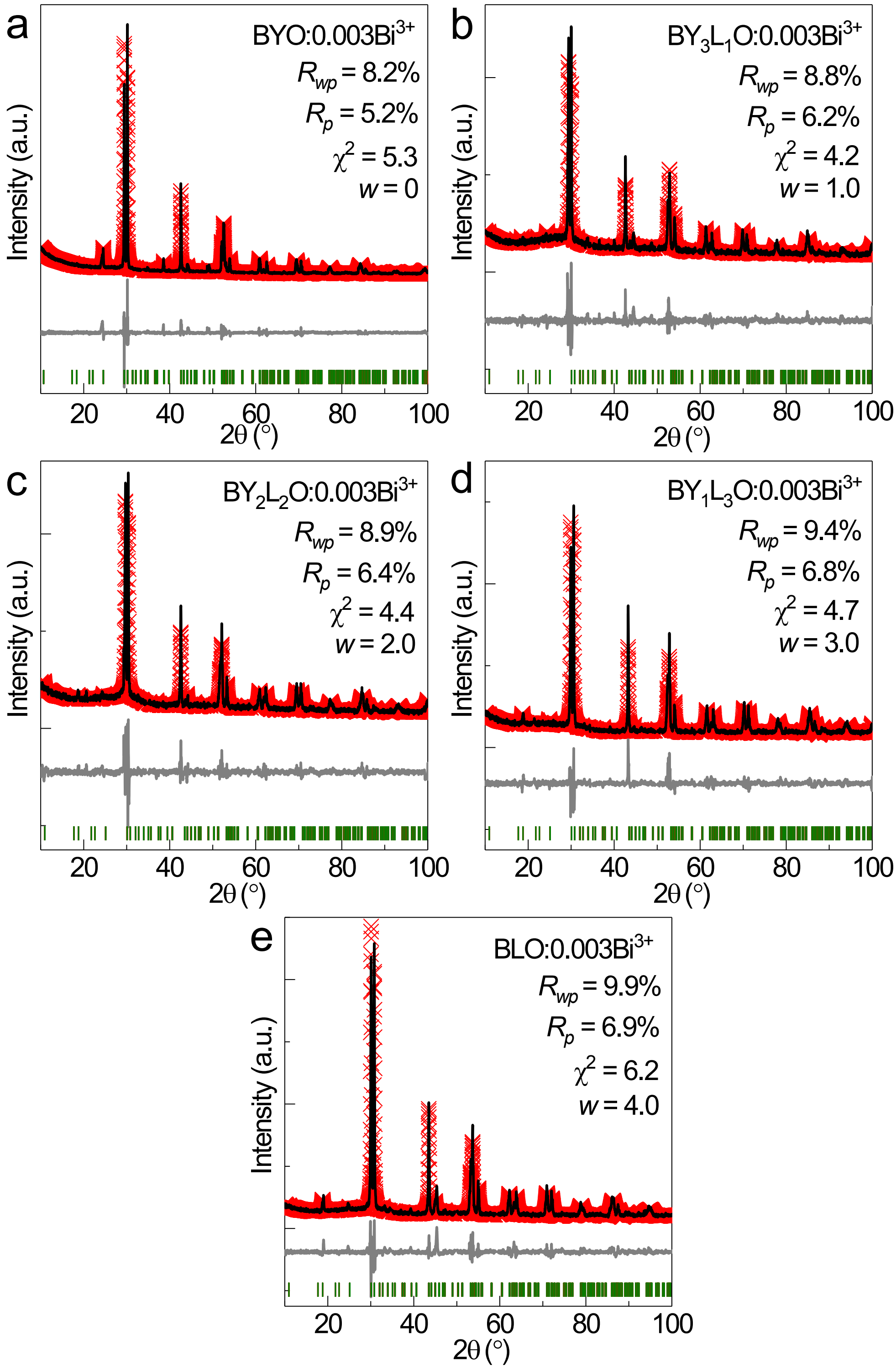

Fig. S1. Rietveld refinement XRD data of $BY_{4\text{-}w}L_wO:Bi^{3+}$ ($0 \leq w \leq 4$) samples, where (a) $BYO:Bi^{3+}$ ($w = 0$), (b) $BY_3L_1O:Bi^{3+}$ ($w = 1$), (c) $BY_2L_2O:Bi^{3+}$ ($w = 2$), (d) $BY_1L_3O:Bi^{3+}$ ($w = 3$) and (e) $BLO:Bi^{3+}$ ($w = 4$) with the measured data (red circle), fitted data (black line), difference (grey line) and Bragg position (olive vertical bar).

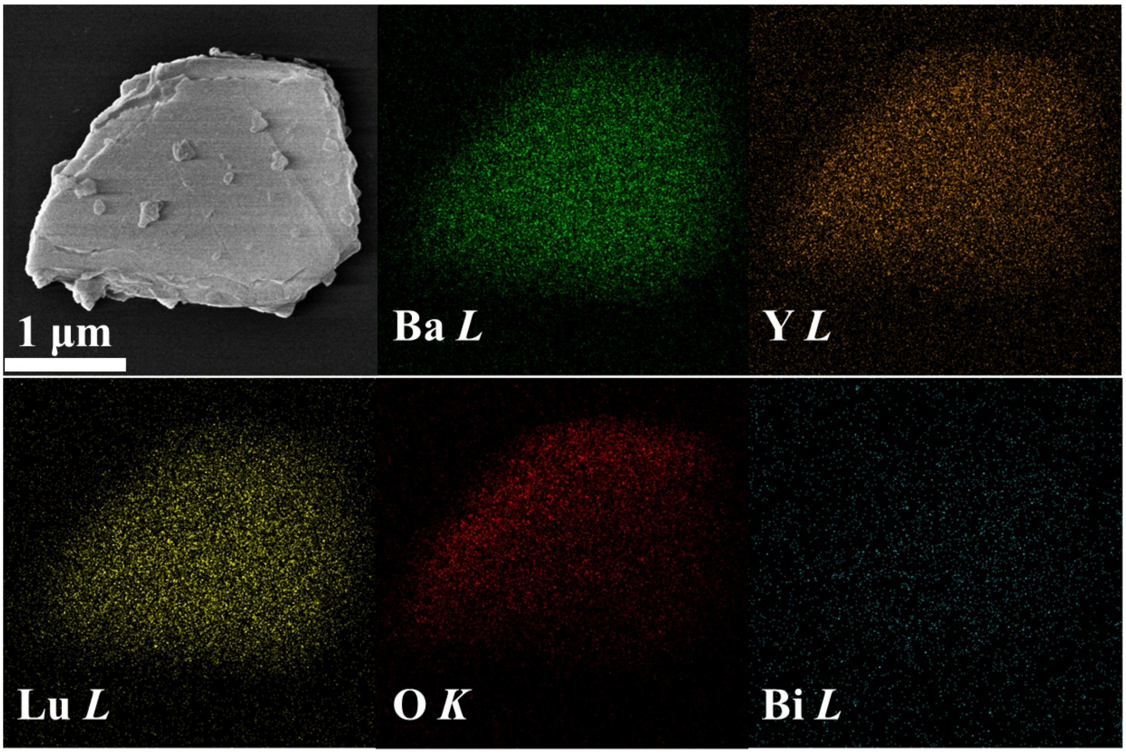

Fig. S2. SEM image and corresponding elemental mapping analysis for Ba, Y, Lu, O and Bi elements in $BY_2L_2O:Bi^{3+}$ (w = 2).

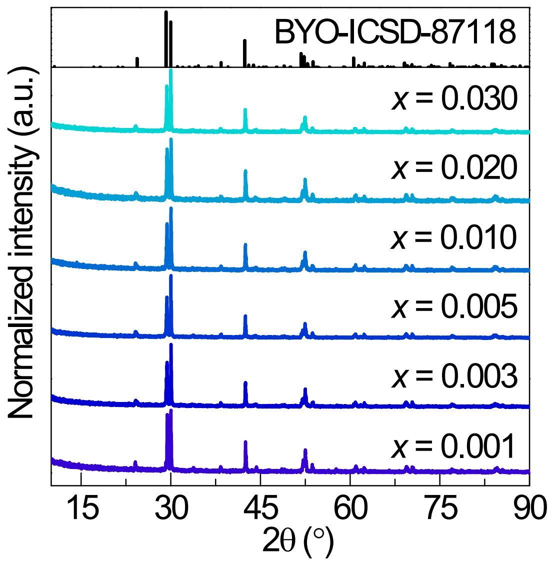

Fig. S3. The XRD patterns of BYO:xBi^{3+} ($0.001 \leq x \leq 0.03$) and the standard data of BYO (ICSD-87118).

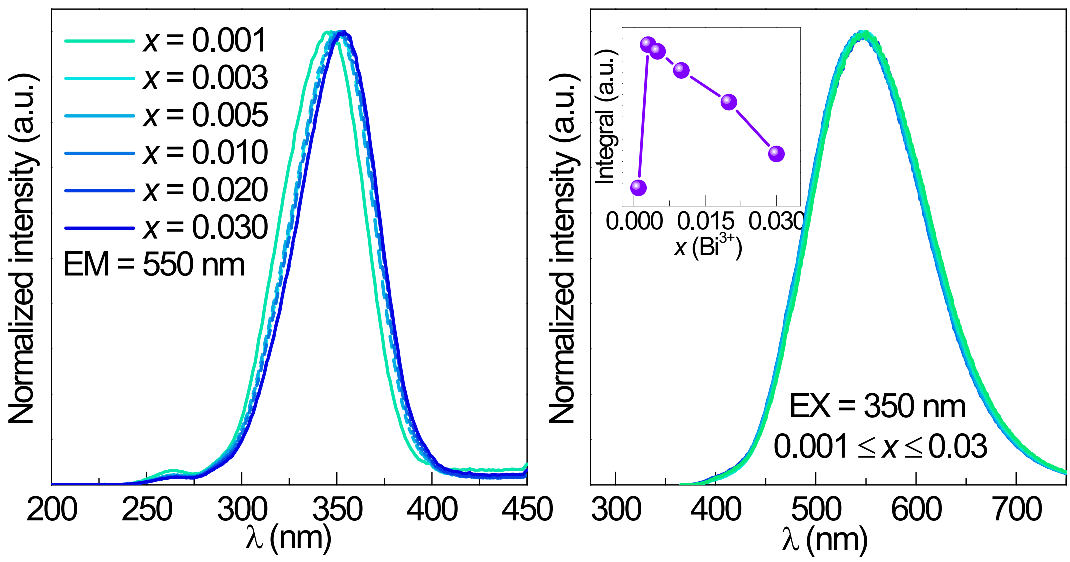

Fig. S4. The normalized (a) PLE spectra (monitoring at 550 nm) and (b) PL spectra (exciting at 350 nm) of BYO:$x$$Bi^{3+}$ ($0.001 \leq x \leq 0.03$), the inset is the integrated intensity of BYO:$x$$Bi^{3+}$ ($0.001 \leq x \leq 0.03$) as a function of Bi^{3+} concentrations (x).

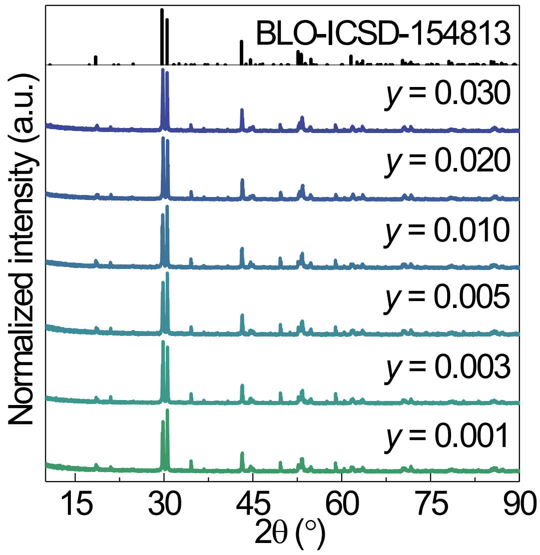

Fig. S5. The XRD patterns of BLO:yBi^{3+} ($0.001 \leq y \leq 0.03$) and the standard data of BLO (ICSD-154813).

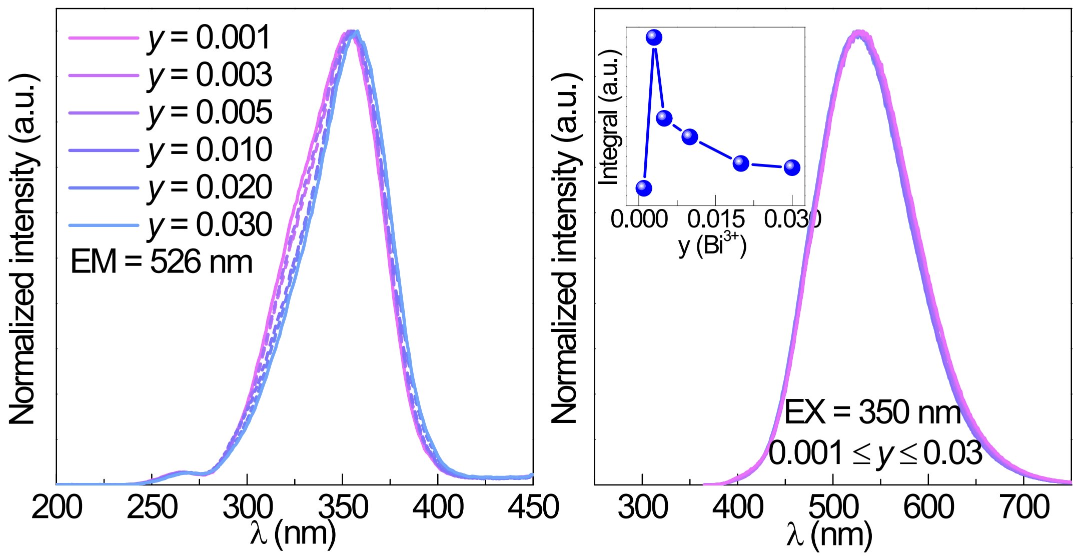

Fig. S6. The normalized (a) PLE spectra (monitoring at 526 nm) and PL spectra (exciting at 350 nm) of BLO:$y$$Bi^{3+}$ ($0.001 \le y \le 0.03$), the inset is the integrated intensity of BYO:$x$$Bi^{3+}$ ($0.001 \le x \le 0.03$) as a function of Bi^{3+} concentrations (y).

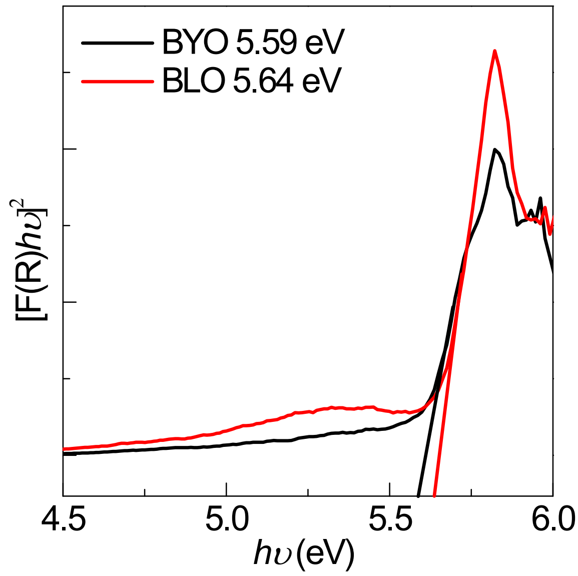

Fig. S7. the relationship of $[F(R)h\nu]^2$ vs photon energy $h\nu$ in BYO and BLO host.

$$[F(R)h\nu]^2 = A\ (h\nu\text{-}Eg),\ F(R) = (1\text{-}R)^2/2R$$

Where A stands for absorption constant, *Eg* represents the optical band gap, *hv* is the photon energy, F(*R*) is the absorption coefficient, and *R* is the reflectance coefficient (%), respectively.

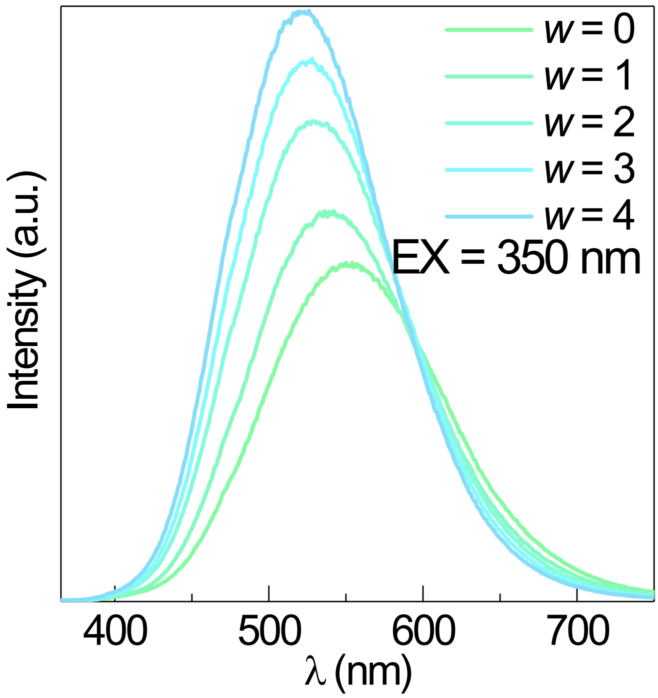

Fig. S8. The PL spectra of the solid solution $BY_{4\text{-}w}L_wO{:}Bi^{3+}$ ($0 \leq w \leq 4$), monitoring at 350 nm.

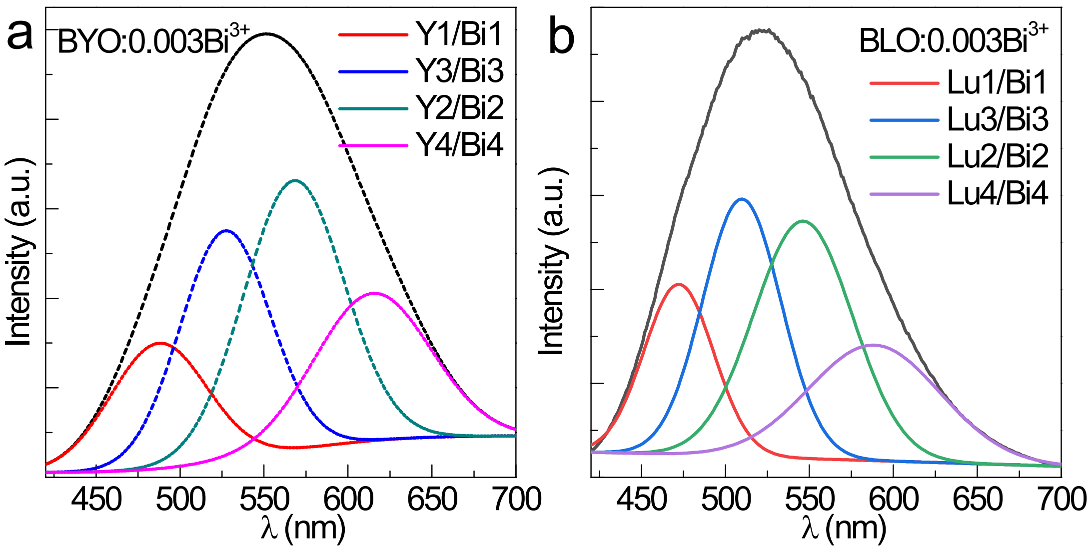

Fig. S9. The Gaussian fitting PL spectra of (a) BYO:Bi^{3+} and (b) BLO:Bi^{3+}.

Table S1. Main parameters of Rietveld refinement for the $BY_{4-w}L_wO:Bi^{3+}$ ($0 \le w \le 4$) samples.

w	Phase	Space group	Cell parameters (Å, Å^3)	R_{wp} R_p (%) χ^2
0	$Ba_3Y_4O_9$:0.003Bi^{3+}	$R3$	$a = b = 6.0935$	8.2
			$c = 25.1835$	5.2
			$V = 809.79$	5.3
1	$Ba_3Y_3Lu_1O_9$:0.003Bi^{3+}	$R3$	$a = b = 6.0681$	8.8
			$c = 25.0796$	6.2
			$V = 798.18$	4.2
2	$Ba_3Y_2Lu_2O_9$:0.003Bi^{3+}	$R3$	$a = b = 6.0214$	8.9
			$c = 24.991$	6.4
			$V = 784.71$	4.4
3	$Ba_3Y_1Lu_3O_9$:0.003Bi^{3+}	$R3$	$a = b = 6.0020$	9.4
			$c = 24.9006$	6.8
			$V = 776.84$	4.7
4	$Ba_3Lu_4O_9$:0.003Bi^{3+}	$R3$	$a = b = 5.9896$	9.9
			$c = 24.7856$	6.9
			$V = 770.06$	6.2

Table S2. The average Y/Lu/Bi-O bonds length of $BY_{4-w}L_wO:Bi^{3+}$ ($0 \le w \le 4$).

	Y1/Lu1/Bi1-O (Å)	Y2/Lu2/Bi2-O (Å)	Y3/Lu3/Bi3-O (Å)	Y4/Lu4/Bi4-O (Å)
$w = 0$	2.3522	2.2483	2.3491	2.2276
$w = 1$	2.3518	2.2384	2.3495	2.2229
$w = 2$	2.3515	2.2282	2.3501	2.2173
$w = 3$	2.3511	2.2191	2.3503	2.2142
$w = 4$	2.3508	2.2112	2.3505	2.2095

Table S3. The average Ba1/Ba2-O bonds length of $BY_{4-w}L_wO:Bi^{3+}$ ($0 \le w \le 4$).

samples		average length (Å)		average length (Å)
$w = 0$	Ba1-O	3.01031	Ba2-O	3.20362
$w = 1$	Ba1-O	2.99918	Ba2-O	3.17141
$w = 2$	Ba1-O	2.95311	Ba2-O	3.08966
$w = 3$	Ba1-O	2.89773	Ba2-O	3.04872
$w = 4$	Ba1-O	2.8118	Ba2-O	2.90135